Supplementary Online Data Repository Entry:

Geology Ms#G22163A

"The Huygens-Hellas Giant Dike System on Mars: Implications for Late Noachian-Early Hesperian Volcanic Resurfacing and Climatic Evolution"

By J. W. Head[1], L. Wilson[2], J. Dickson[1], G. Neukum[3] and the HRSC Team.
[1]Department of Geological Sciences, Brown University, Providence, RI 02912 USA; [2]Environmental Science Department, Lancaster University, Lancaster LA1 4YQ, UK; [3]Institut fuer Geologische Wissenschaften, Freie Universitaet Berlin, Malteserstrasse 74-100, 12249 Berlin, Germany.

Submitted 8/11/05; Revised version submitted 11/29/05

Mars Chronology

The geological time scale of Mars is based on stratigraphic relationships (e.g., Tanaka et al., 1992) and impact crater size-frequency distribution on specific mapped units (e.g., Hartmann and Neukum, 2001). The geological time scale of Mars is subdivided into three periods, the Noachian, from ~4.5 to ~3.7 Gyr ago, the Hesperian, extending from ~3.0 to ~3.7 Gyr ago, and the Amazonian, from ~3.7 Gyr ago to the present. Synthesis global 1:15 M scale geological maps of Mars can be found in Greeley and Guest (1987) and Scott and Tanaka (1986).

Mars Geological Mapping and Interpretation of Units

Synthesis geological maps of Mars (Greeley and Guest, 1987; Scott and Tanaka, 1986) are compiled from interpretation and mapping of features and units seen in images and topography. A general introduction to planetary data and mapping techniques can be found in Greeley and Batson (1997) and descriptions of mapping techniques and major geological units for Mars can be found in Carr (1981), Greeley and Batson (1997) and Tanaka et al. (1992).

Recent Spacecraft Data for Mars

A host of missions to Mars have been launched in the last decade and much of the resulting data have been utilized in this study. We used data from the following missions and instruments and the URL for each is provided below.

Mars Global Surveyor Mission: URL http://marsprogram.jpl.nasa.gov/mgs/
-MOC-Mars Orbiter Camera: URL http://www.mss.com/mgs/moc/index.html
-MOLA-Mars Orbiter Laser Altimeter: URL
http://ltpwww.gsfc.nasa.gov/tharsis/mola.html
-MOLA PEDR (Precision Experiment Data Record): URL http://pds-geosciences.wustl.edu/missions/mgs/pedr.html

Mars Odyssey Mission: URL http://marsprogram.jpl.nasa.gov/odyssey/
-THEMIS-Thermal Emission Imaging System: URL http://themis.asu.edu

Mars Express Mission: URL http://www.esa.int'/SPECIALS/Mars_Express/index.html
-HRSC (High Resolution Stereo Camera): URL
http://solarsystem.dlr.de/Missions/express/indexeng.shtml

Images of Extrusive Components of Dike Emplacement

Dike emplacement events result in the intrusion of blade-like magma-filled fractures in the crust, extending from the source region toward the surface. Dike emplacement events are predominantly intrusive with depth and along strike, but occasionally they extend locally to the surface to form eruptions. The surface morphology of those that reach the surface on both Earth and Mars are readily distinguished in terms of morphology from those that are in the subsurface and have been exhumed. Where dikes reach the surface, they form spatter and cinder cones, and flows (Head et al., 2005) (Fig. 1). Where they are exhumed, they form continuous ridges and flanking debris aprons such as those seen at Ship Rock, New Mexico USA.

Calculations on the Nature and Eruption Properties of Buried Dikes

The geometry and extent of the observed ridges provide important constraints on the nature of the dikes and the eruption conditions that might have accompanied their emplacement. The broad ridge in lower resolution images is typically ~700 m across and the details revealed in high-resolution images suggest that the surface exposure of the ridge crest is ~60 m wide. Using analytical expressions for the cross-sectional shapes of dikes containing buoyant magma developed by Weertman (1971), the width W of a dike as a function of depth L below its upper tip can be written as

$$W = [(1-\nu)/\mu]\ (2/3)\ \Delta P\ [8\ A\ L]^{1/2}$$

where A is the half-height of the dike, ΔP is the internal excess pressure and ν and μ are the Poisson's ratio and shear modulus for the host rocks, respectively. For giant dikes on Mars, Wilson and Head (2002a) found typically A = 30 km and ΔP = 40 MPa. Likely crustal values of ν and μ are 0.25 and 5 GPa, respectively (Parfitt, 1991; Rubin 1993), implying the following variation of W with L.

depth, L, below top of dike in km	dike width, W, in m
0	0
0.5	44
1	62
2	88
3	108
5	138
10	196
20	276
30	340
	mean width: 226

Thus, the ratio of mean dike width to dike width at 500 m depth is 5.1, so an observed 60 m width at an assumed depth of erosion of 500 m would imply a mean dike width of 306

m. If the erosion depth was 1 km, the ratio is 3.6 and the implied mean dike width would be 216 m. Mean dike widths of order 200-300 m correspond to dikes whose tops are located between zero (the part that erupts) and as much as several hundreds of meters (Figure 14b in Wilson and Head, 2002).

References

Carr, M., 1981, *The Surface of Mars*: Yale Univ. Press, New London, 232 p.

Greeley, R. and Batson, R., 1997, The NASA Atlas of the Solar System, Cambridge Univ. Press, Cambridge, 369 p.

Greeley, R. and Guest, J., 1987, Geologic map of the eastern equatorial region of Mars: USGS Miscellaneous Investigations Series Map I-1802-B, scale 1:15,000,000, 1 sheet.

Head, J., Shean, D., and Wilson, L., 2005, Post-glacial dike emplacement event at Arsia Mons, Mars: Eruptive spatter cones, tephra cones and flows along a dike-related fissure: Brown Univ.-Vernadsky Inst. Microsymposium 42, CD-ROM, Abstract #22.

Hartmann, W. and Neukum, G., 2001, Cratering chronology and the evolution of Mars, Space Sci. Rev., v. 96, p. 163-194.

Parfitt, E., 1991, The role of rift-zone storage in controlling the site and timing of eruptions and intrusions of Kilauea volcano, Hawai'i: J. Geophys. Res., v. 96, p. 10101-10112.

Rubin, A., 1992, Dike-induced faulting and graben subsidence in volcanic rift zones: J. Geophys. Res., v. 97, p. 1839-1858.

Scott, D., and Tanaka, K., 1986, Geologic map of the western equatorial region of Mars: USGS Miscellaneous Investigations Series Map I-1802-B, scale 1:15,000,000, 1 sheet.

Tanaka, K., Scott, D., and Greeley, R., 1992, Global stratigraphy; in *Mars*, H. Kieffer et al., eds., Univ. Ariz. Press, Tucson, p. 345-382.

Weertman, J., 1971, Theory of water-filled crevasses in glaciers applied to vertical magma transport beneath oceanic ridges: J. Geophys. Res., v. 76, p. 1171-1183.

Wilson, L., and Head, J., 2002, Tharsis-radial graben systems as the surface manifestation of plume-related dike intrusion complexes: Models and implications: J. Geophys. Res., v. 107 (E8), doi: 10.1029/2001JE001593.

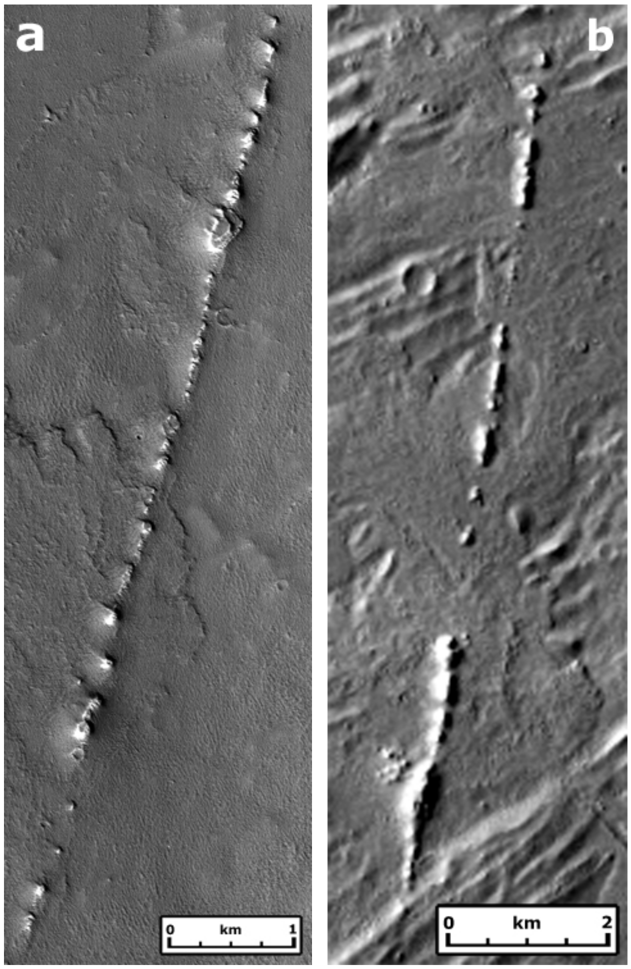

Figure 1. Rows of volcanic cones and adjacent flows superposed on the Arsia Mons fan-shaped cold-based glacial deposit on Mars: A) Southern segment (MOC image S07-01314, 3.5 m/pxl). B) Northern segment (THEMIS image V12087009, 35 m/pxl). From Head et al. (2005).